

# Elastic and Viscoelastic Properties of Non-bulk Polymer Interphases in Nanotube-reinforced Polymers

Frank T. Fisher<sup>1</sup>, Kon-Chol Lee<sup>1</sup>, and L. Catherine Brinson<sup>2</sup>

<sup>1</sup>Department of Mechanical Engineering, Stevens Institute of Technology  
Castle Point on Hudson, Hoboken, NJ 07030

<sup>2</sup>Departments of Mechanical Engineering and Materials Science and Engineering  
Northwestern University, 2145 Sheridan Road, Evanston, IL 60208

## ABSTRACT

There is considerable interest in using carbon nanotubes (NTs) to create multifunctional polymer composite materials with outstanding mechanical, electrical, and thermal properties. A hurdle in modeling the behavior of these systems is the non-bulk interphase region in these systems that forms due to nanoscale interactions between the embedded NTs and adjacent polymer chains. This interphase region comprises a substantial portion of the volume fraction of the composite due to the tremendous NT surface area per unit volume available for interaction with local polymer chains and results in significant changes in the viscoelastic properties of the nanotube-polymer composite compared to those of the bulk polymer. However, the mechanical properties of this interphase region are unknown and very difficult to measure directly from experimental testing due to the size scale of this interphase region. Thus a three-phase (fiber/nanotube – annular interphase – matrix) Mori-Tanaka micromechanical model has been developed such that the properties of this interphase region can be inferred from macroscale viscoelastic data obtained using dynamic mechanical analysis. Such analysis will be particularly useful as a means to assess changes in the mobility and mechanical behavior of this interphase region and as a means to characterize the impact of chemical functionalization on interphase formation in these systems.

## BACKGROUND

Due to the inherent strength of the carbon-carbon bond and the potential of a defect-free structure, it has been suggested that nanotubes may approach the theoretical limits for many important mechanical properties, including axial stiffness and tensile strength. Large increases in fracture strain and toughness, and superior electrical/thermal properties, are other potential benefits of using NTs as the filler material in a polymer-based composite. Detailed discussions of the mechanical properties of nanotubes and their use in composites are provided in a number of places in the literature; see for example [1, 2] and [3, 4], respectively.

Efforts to model the mechanical behavior of nanotube-polymer composites are complicated by the presence of a polymeric interphase region surrounding the nanotubes with properties different from that of the matrix polymer. While first postulated based on changes in the viscoelastic behavior of nanotube-polymer composites in comparison to the behavior of the pure matrix polymer material, a number of recent computational atomistic modeling results are consistent with the presence of this interphase region [5-7]. For at least some nanotube-polymer systems, this interphase polymer has been characterized as having restricted molecular mobility due to the impeded molecular motion of those polymer chains interacting with the embedded nanotubes. Such restricted molecular mobility within the interphase region has been inferred experimentally in a number of ways, including: shifting of the nanocomposite glass transition temperature to higher temperatures [8, 9], broadening of the loss tangent peak [10], changes in the relaxation spectra [11], and formation of a strongly adhered polymer layer on the surface of the nanotubes [12]. Chemical functionalization of the nanotubes and subsequent covalent tethering of short-chain polymers to the nanotube surface has been shown to increase the interphase effect in nanotube-polymer composites [13, 14].

## INTRODUCTION TO THE MORI-TANAKA METHOD FOR MULTIPHASE COMPOSITES

The Mori-Tanaka method is a popular micromechanics tool for the study of multiphase materials; the reader is referred to the literature for an in-depth derivation and discussion of the method [15-17]. A critical component of the Mori-Tanaka method is

the determination of the dilute strain concentration tensor  $A_r^{dil}$ , which relates the average strain of the  $r$ th inclusion to the far-field strain in the matrix  $\bar{\epsilon}_0$  such that

$$\bar{\epsilon}_r = A_r^{dil} \bar{\epsilon}_0. \quad (1)$$

If such a tensor can be determined, one can show that the effective stiffness of a composite with randomly oriented inclusions can be written as [17]

$$C = \left( f_0 C_0 + \sum_{n=1}^r f_n \{ C_n A_n^{dil} \} \right) \left( f_0 I + \sum_{n=1}^r f_n \{ A_n^{dil} \} \right)^{-1}, \quad (2)$$

where  $C$  is the effective stiffness tensor of the composite,  $f_r$  and  $C_r$  are the volume fraction and stiffness of inclusion phase  $r$ ,  $f_0$ , and  $C_0$  are the volume fraction and stiffness of the matrix material,  $I$  is the identity tensor, and brackets  $\{ \}$  denote the appropriate orientational average (see [18]). The ability to handle spatial orientation distributions of the embedded nanotubes within the polymer is critical, as the nanotubes are rarely aligned within polymer nanocomposites. For inclusions which are ellipsoidal in shape, the solution for the dilute strain concentration tensor  $A_r^{dil}$  can be written explicitly in terms of the Eshelby tensor  $S_r$ , which for an isotropic matrix is only a function of the inclusion shape and the Poisson ratio of the matrix, such that

$$A_r^{dil} = [I + S_r C_0^{-1} (C_r - C_0)]^{-1}. \quad (3)$$

General forms for the Eshelby tensor for ellipsoidal inclusions [19], including the limit case of infinitely long cylindrical inclusions [20], are provided in the literature.

As shown in Figure 1A, the standard multiphase Mori-Tanaka approach requires separate, physically distinct ellipsoidal inclusion phases for the calculation of the Eshelby tensor of each phase for substitution into (3). Thus, while one could model a three phase nanocomposite (bulk polymer as the matrix phase and interphase polymer and nanotube as the inclusion phases), such an approach represents a physical system as in Figure 1A where the interphase is a separate ellipsoidal inclusion from the nanotube inclusions. However, the actual physical geometry of nanotube-reinforced polymer systems is such that the interphase region is an annular region, continuous with and surrounding the nanotube (see Figure 1B). Thus, the development of the dilute strain concentration tensor for coated fibers is needed, as presented in the next section. Note that the simplified model shown in Figure 1A has been used previously by the authors to model the mechanical behavior of viscoelastic interphases [21] and the mechanical behavior of a nanotube-reinforced polymers [14, 22]. Therefore the results of this work will also clarify the degree of error in this approximation and help to define conditions under which accurate representation of the annular interphase is essential. In the next section of the paper, an analytical method is used to derive the dilute strain concentration tensors for the nanotube and its continuous annular interphase, respectively, via the definition in (1). Subsequently, these tensors can be substituted directly into (2) to determine the effective stiffness of the nanotube-reinforced polymer. Such example calculations are then provided in the Results section.

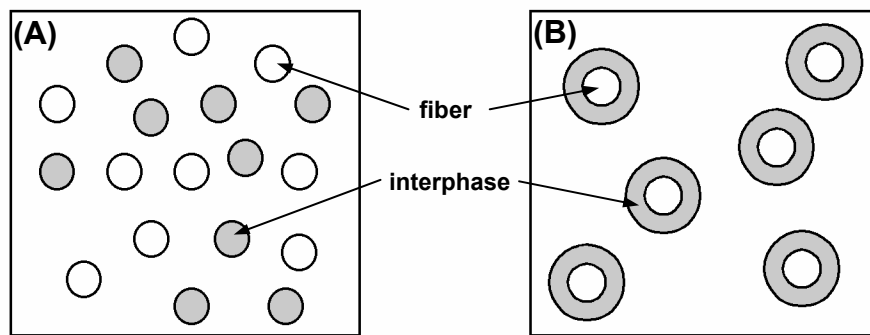


**Figure 1. Schematic of micromechanics approaches. (A) Standard multiphase Mori-Tanaka approach. (B) Coated fibrous inclusion approach.**

## DILUTE STRAIN CONCENTRATION FOR INFINITELY LONG COATED INCLUSIONS

Several micromechanics-based models have been developed to determine the effective moduli of composites with coated inclusions. A number of these methods (including the present) are based on the analytical solution for the stress fields in an infinitely long coated fiber first developed by Benveniste and co-workers for aligned inclusions [23]. For example, Weng and co-workers developed an iterative approach where a two-phase composite is modeled using a three-phase inclusion-matrix-effective composite geometry in terms of a modified Eshelby tensor to account for particle interactions at high concentrations of inclusions [20, 24]. Alternative micromechanics approaches, such as one developed specifically for thickly coated inclusions based on a progressively filled composite element assembly [25], have also been developed.

The approach presented here is a re-formulation of the original Benveniste method, where for reasons discussed previously we solve explicitly for the dilute strain concentration tensors for the fiber and interphase regions using the definition in (1). Such an approach is related our previous work, where the components of the dilute strain concentration tensor were calculated directly using the finite element method to model the impact of nanotube waviness on the effective modulus of a two phase nanotube-polymer composite [26].

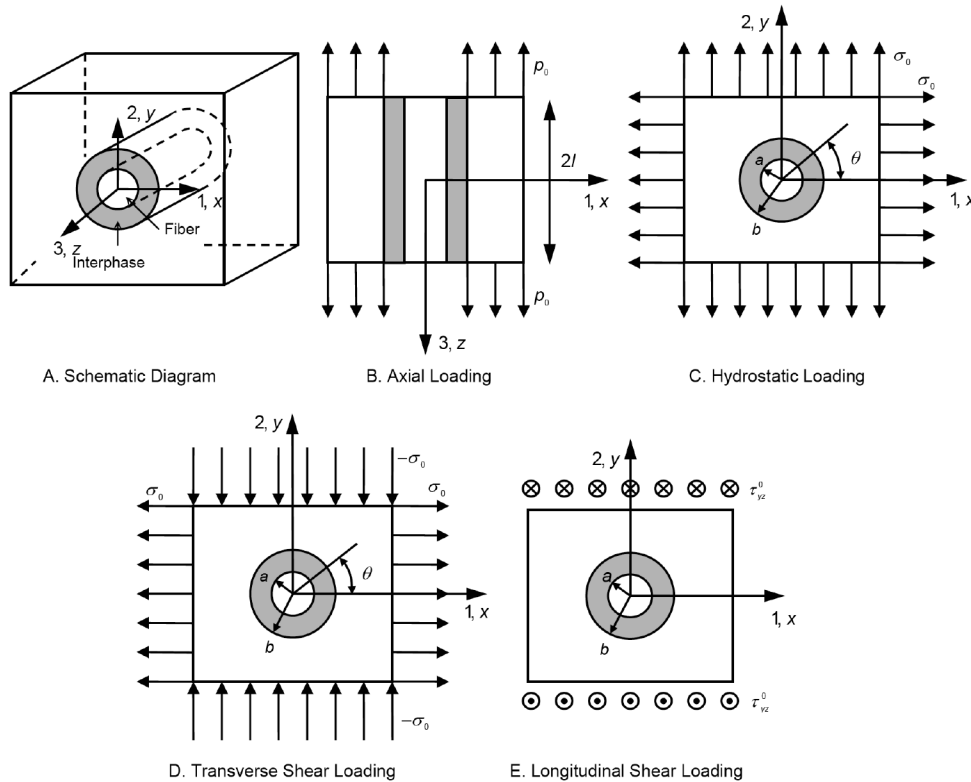


**Figure 2. (A) Determination of dilute strain concentration based on a single coated fibrous inclusion in an infinite matrix material. (B) Axial loading case. (C) Hydrostatic loading case. (D) Transverse shear loading. (E) Longitudinal shear loading.**

Using contracted notation, the dilute strain concentration tensors given in (1) can be written explicitly for the fiber<sup>1</sup> and interphase, respectively, as

<sup>1</sup> Because the micromechanics approach presented here assumes a continuum description for the mechanical behavior of the nanotube, the terms *nanotube* and *fiber* are used interchangeably.

$$A_r^{dil} = \begin{bmatrix} A_r^{11} & A_r^{12} & A_r^{13} & 0 & 0 & 0 \\ A_r^{21} & A_r^{22} & A_r^{23} & 0 & 0 & 0 \\ A_r^{31} & A_r^{32} & A_r^{33} & 0 & 0 & 0 \\ 0 & 0 & 0 & A_r^{44} & 0 & 0 \\ 0 & 0 & 0 & 0 & A_r^{55} & 0 \\ 0 & 0 & 0 & 0 & 0 & A_r^{66} \end{bmatrix}, \quad A_g^{dil} = \begin{bmatrix} A_g^{11} & A_g^{12} & A_g^{13} & 0 & 0 & 0 \\ A_g^{21} & A_g^{22} & A_g^{23} & 0 & 0 & 0 \\ A_g^{31} & A_g^{32} & A_g^{33} & 0 & 0 & 0 \\ 0 & 0 & 0 & A_g^{44} & 0 & 0 \\ 0 & 0 & 0 & 0 & A_g^{55} & 0 \\ 0 & 0 & 0 & 0 & 0 & A_g^{66} \end{bmatrix}. \quad (4)$$

The goal of the current work is to develop an analytical solution for each of the individual components of the dilute strain concentration tensors given in (4). First, using (1) with (4) one finds that

$$\bar{\varepsilon}_{33}^f = A_f^{31} \bar{\varepsilon}_{11}^m + A_f^{32} \bar{\varepsilon}_{22}^m + A_f^{33} \bar{\varepsilon}_{33}^m, \quad \bar{\varepsilon}_{33}^g = A_g^{31} \bar{\varepsilon}_{11}^m + A_g^{32} \bar{\varepsilon}_{22}^m + A_g^{33} \bar{\varepsilon}_{33}^m. \quad (5)$$

By inspection, for the case of an infinitely long coated inclusion embedded in an infinite matrix considered here, the average axial strain in the fiber and interphase regions ( $\bar{\varepsilon}_{33}^r$ ;  $r = f, g$ ) will be independent of the transverse strains of the matrix and equal to the axial component of the matrix strain. Thus

$$\begin{aligned} A_f^{31} = A_f^{32} = A_g^{31} = A_g^{32} &= 0 \\ A_f^{33} = A_g^{33} &= 1 \end{aligned}, \quad (6)$$

such that the dilute strain concentration tensors can be further simplified to

$$A_r^{dil} = \begin{bmatrix} A_r^{11} & A_r^{12} & A_r^{13} & 0 & 0 & 0 \\ A_r^{21} & A_r^{22} & A_r^{23} & 0 & 0 & 0 \\ 0 & 0 & 1 & 0 & 0 & 0 \\ 0 & 0 & 0 & A_r^{44} & 0 & 0 \\ 0 & 0 & 0 & 0 & A_r^{55} & 0 \\ 0 & 0 & 0 & 0 & 0 & A_r^{66} \end{bmatrix}, \quad A_g^{dil} = \begin{bmatrix} A_g^{11} & A_g^{12} & A_g^{13} & 0 & 0 & 0 \\ A_g^{21} & A_g^{22} & A_g^{23} & 0 & 0 & 0 \\ 0 & 0 & 1 & 0 & 0 & 0 \\ 0 & 0 & 0 & A_g^{44} & 0 & 0 \\ 0 & 0 & 0 & 0 & A_g^{55} & 0 \\ 0 & 0 & 0 & 0 & 0 & A_g^{66} \end{bmatrix}. \quad (7)$$

In addition, as shown in Figure 2A, one can take advantage of the symmetry of the 1-2 plane to further simplify the dilute strain concentration tensors given in (7), i.e.

$$A_r^{dil} = \begin{bmatrix} A_r^{11} & A_r^{12} & A_r^{13} & 0 & 0 & 0 \\ A_r^{12} & A_r^{11} & A_r^{13} & 0 & 0 & 0 \\ 0 & 0 & 1 & 0 & 0 & 0 \\ 0 & 0 & 0 & A_r^{44} & 0 & 0 \\ 0 & 0 & 0 & 0 & A_r^{44} & 0 \\ 0 & 0 & 0 & 0 & 0 & A_r^{66} \end{bmatrix}, \quad A_g^{dil} = \begin{bmatrix} A_g^{11} & A_g^{12} & A_g^{13} & 0 & 0 & 0 \\ A_g^{12} & A_g^{11} & A_g^{13} & 0 & 0 & 0 \\ 0 & 0 & 1 & 0 & 0 & 0 \\ 0 & 0 & 0 & A_g^{44} & 0 & 0 \\ 0 & 0 & 0 & 0 & A_g^{44} & 0 \\ 0 & 0 & 0 & 0 & 0 & A_g^{66} \end{bmatrix}, \quad (8)$$

such that there are now five independent components ( $A_r^{11}, A_r^{12}, A_r^{13}, A_r^{44}, A_r^{66}$ ;  $r = f, g$ ) of the dilute strain concentration tensor for each inclusion phase.

The remaining components of the dilute strain concentration tensors are found via the analytical solution of the average strains in the fiber and interphase regions for the loading cases shown in Figure 2B-2E following the analysis of Benveniste [23]. The general solution procedure is as follows: for each of these loading cases, one can write the appropriate forms of the displacements of each phase as a function of position in terms of unknown constants. Given these displacements, strain-displacement relationships and Hooke's Law are invoked to determine the strains and stresses in each phase. Appropriate boundary conditions are then invoked, which allows one to determine the unknown constants in the displacement (and hence strain and stress) fields, thus providing the analytical solution for each loading case. From these analytical solutions, the phase-averaged strains for the fiber and the interphase can be determined, at which point the components of the dilute strain concentration tensor for each phase as defined in (1) can be determined.

To illustrate the procedure, we will consider the solution of the longitudinal shear loading case shown in Figure 2E, which will provide the analytical solution for  $A_f^{44}$  and  $A_g^{44}$  in (8). A more detailed presentation of this derivation, as well as the derivation

for the other loadings cases shown in Figure 2 will be presented elsewhere [27]. For this loading case, the non-zero displacements can be written as

$$\begin{aligned} u_z^f &= A_{f4} r \sin \theta \\ u_z^g &= \left( A_{g4} r + \frac{B_{g4}}{r} \right) \sin \theta \\ u_z^m &= \left( A_{m4} r + \frac{B_{m4}}{r} \right) \sin \theta \end{aligned} \quad (9)$$

where  $A_{f4}$ ,  $A_{g4}$ ,  $B_{g4}$ ,  $A_{m4}$ , and  $B_{m4}$  are unknown constants to be determined. Non-zero strain components in cylindrical coordinates are given as

$$\begin{aligned} \varepsilon_{rz}^f &= A_{f4} \sin \theta, \quad \varepsilon_{rz}^g = \left( A_{g4} - \frac{B_{g4}}{r^2} \right) \sin \theta, \quad \varepsilon_{rz}^m = \left( A_{m4} - \frac{B_{m4}}{r^2} \right) \sin \theta \\ \varepsilon_{z\theta}^f &= A_{f4} \cos \theta, \quad \varepsilon_{z\theta}^g = \left( A_{g4} + \frac{B_{g4}}{r^2} \right) \cos \theta, \quad \varepsilon_{z\theta}^m = \left( A_{m4} + \frac{B_{m4}}{r^2} \right) \cos \theta \end{aligned} \quad (10)$$

Using Hooke's Law, the non-zero stress components can be written as

$$\begin{aligned} \sigma_{rz}^f &= 2\mu_f A_{f4} \sin \theta, \quad \sigma_{rz}^g = 2\mu_g \left( A_{g4} - \frac{B_{g4}}{r^2} \right) \sin \theta, \quad \sigma_{rz}^m = 2\mu_m \left( A_{m4} - \frac{B_{m4}}{r^2} \right) \sin \theta \\ \sigma_{z\theta}^f &= 2\mu_f A_{f4} \cos \theta, \quad \sigma_{z\theta}^g = 2\mu_g \left( A_{g4} + \frac{B_{g4}}{r^2} \right) \cos \theta, \quad \sigma_{z\theta}^m = 2\mu_m \left( A_{m4} + \frac{B_{m4}}{r^2} \right) \cos \theta \end{aligned} \quad (11)$$

The above stress fields can be converted to Cartesian coordinates using the relationship  $\sigma_{yz}^r = \sigma_{rz}^r \sin \theta + \sigma_{z\theta}^r \cos \theta$  ( $r = f, g, m$ ). Appropriate boundary conditions for the given case are

$$\begin{aligned} u_z^f &= u_z^g, \quad \sigma_{rz}^f = \sigma_{rz}^g & \text{at } r = a \\ u_z^g &= u_z^m, \quad \sigma_{rz}^g = \sigma_{rz}^m & \text{at } r = b, \\ \varepsilon_{yz}^m &= \varepsilon_{yz}^0 & \text{as } r \rightarrow \infty \end{aligned} \quad (12)$$

the application of which can be shown to yield the following system of equations (in matrix form) which can be solved to find the unknown field constants in (9)-(11).

$$\begin{bmatrix} a & -a & -\frac{1}{a} & 0 & 0 \\ 0 & b & \frac{1}{b} & -b & -\frac{1}{b} \\ \mu_{yz}^f & -\mu_{yz}^g & \frac{\mu_{yz}^g}{a^2} & 0 & 0 \\ 0 & \mu_{yz}^g & -\frac{\mu_{yz}^g}{a^2} & -\mu_{yz}^m & \frac{\mu_{yz}^m}{b^2} \\ 0 & 0 & 0 & 1 & 0 \end{bmatrix} \begin{bmatrix} A_{f4} \\ A_{g4} \\ B_{g4} \\ A_{m4} \\ B_{m4} \end{bmatrix} = \begin{bmatrix} 0 \\ 0 \\ 0 \\ 0 \\ \varepsilon_{yz}^0 \end{bmatrix} \quad (13)$$

Once the known constants  $A_{f4}$ ,  $A_{g4}$ ,  $B_{g4}$ ,  $A_{m4}$ ,  $B_{m4}$  have been determined via (13), their substitution into (10) provides analytical expressions for the strain fields for each phase in the composite. The phase averaged strain components in the fiber and inclusion phases can then be determined using

$$\bar{\varepsilon}_{yz}^f = \frac{\int_0^{2\pi} \int_0^a \varepsilon_{yz}^f(r, \theta) r dr d\theta}{\pi a^2}, \quad \bar{\varepsilon}_{yz}^g = \frac{\int_0^{2\pi} \int_a^b \varepsilon_{yz}^g(r, \theta) r dr d\theta}{\pi (b^2 - a^2)}. \quad (14)$$

Likewise, the far-field strain in the matrix for the case of a single infinitely long fiber in an infinite matrix can be determined from (10) as

$$\bar{\varepsilon}_0 = \varepsilon_{yz}^m \Big|_{r \rightarrow \infty} = A_{m4}. \quad (15)$$

Thus, by the definition in (1) the following components of the dilute strain concentration tensors for the fiber and interphase can be determined based on examination of the longitudinal shear case presented above:

$$A_r^{44} = \frac{A_{r4}}{A_{m4}}, \quad A_g^{44} = \frac{A_{g4}}{A_{m4}}, \quad (16)$$

where the values of  $A_{f4}$ ,  $A_{g4}$ , and  $A_{m4}$  are found from the solution to (13).

The remaining dilute strain concentration terms (for both the fiber and the interphase) in (8) can be found via analysis of the loading cases given in Figure 2 as follows:

- $A^{66}$  from the transverse shear loading case (Figure 2D)
- $A^{11}$  and  $A^{12}$  from the transverse hydrostatic loading case given in Figure 2C, with the additional constraint that  $A^{11} - A^{12} = A^{66}$
- $A^{13}$  from a superposition of the axial loading case (Figure 2B) and the transverse hydrostatic case (Figure 2C)

While the solution to the remaining dilute strain concentration terms given in (8) follows the outline of the procedure outlined above, the algebra is unwieldy and will be presented elsewhere [27].

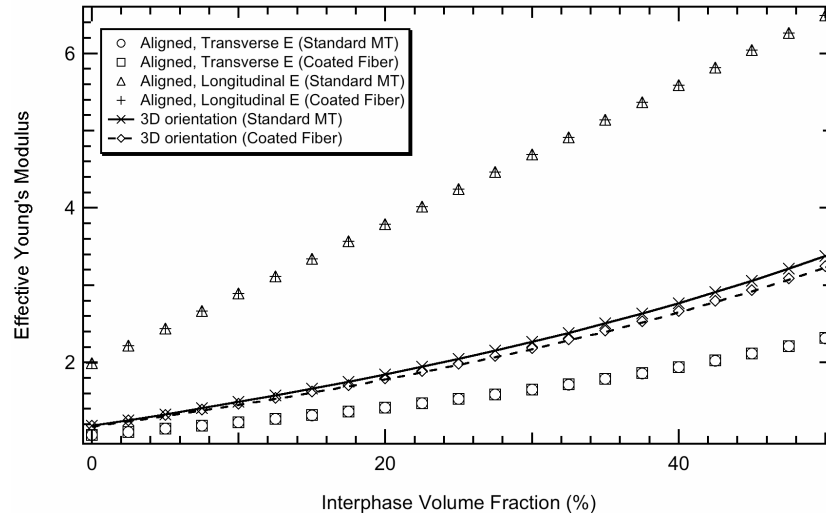
## RESULTS

One can show that the resulting dilute strain concentration tensors for the coated fibrous composite determined in this fashion are identical to those calculated using the Eshelby tensor via (2) for a two phase composite when the interphase properties match those of the fiber or the matrix, respectively.

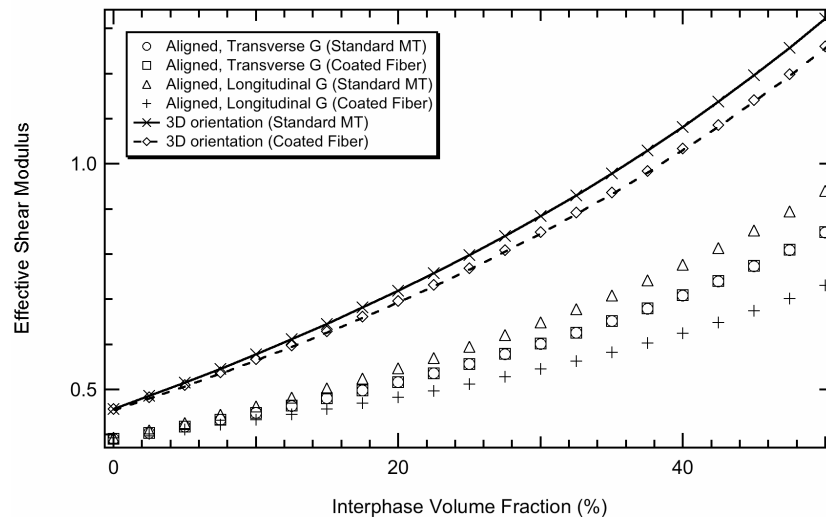
Preliminary results comparing the effective Young's moduli and shear moduli predictions for a three phase composite using the standard Mori-Tanaka implementation (assuming physically distinct fiber and interphase regions; see Figure 1A) and the coated fibrous inclusion model presented here are shown in Figures 3 and 4, respectively. Constant dimensionless Young's moduli of 100, 10, and 1 were chosen for the fiber, interphase, and matrix, respectively. Here the volume fraction of the fiber was kept constant at 1%, while the volume fraction of the interphase varied from 0 to 50%. For all phases a Poisson ratio of 0.3 was assumed. Two types of composites were considered: composites where the fiber and interphase regions are aligned, and a composite with the fiber and interphase regions randomly orientated in 3D space.

Figure 3 shows that there is relatively little difference in the composite moduli predictions between the two methods for the values of elastic moduli shown here. This is not surprising for the aligned composite case, where for infinitely long fibers micromechanical methods approach the simple rule of mixture approximations. More surprisingly, for the case of randomly orientated inclusions in 3D space there is relatively little difference between the standard Mori-Tanaka multiphase analysis and the coated inclusion model presented here for the phase properties assumed here. As shown in Figure 4, there appears to be a larger difference between the methods when evaluating the effective shear modulus of the composites. Further analysis of the differences between the two methods is ongoing.

Note also that, for nanotube-polymer composites with one of the viscoelastic phases close to the glass-rubber transition, it may be possible for the differences in the phase moduli to be much larger than those assumed here. Thus, via implementation of the dynamic correspondence principle to the elastic model developed here, differences in effective viscoelastic moduli predictions between the standard Mori-Tanaka multiphase model and the coated inclusion model will be investigated in detail in future work. Ultimately, given the viscoelastic properties of the bulk matrix material and the effective behavior of the nanocomposite, it will be possible to infer the viscoelastic properties of the interphase region necessary to match the results of the micromechanical modeling with experimental data.



**Figure 3. Effective Young's modulus as a function of interphase volume fraction for different fiber orientations. Fiber:  $E_f = 100$ ,  $v_f = 1\%$ . Interphase:  $E_g = 10$ . Matrix:  $E_m = 1$ . All phases considered isotropic with Poisson's ratio = 0.3.**



**Figure 4. Effective shear modulus as a function of interphase volume fraction for different fiber orientations. Fiber:  $E_f = 100$ ,  $v_f = 1\%$ . Interphase:  $E_g = 10$ . Matrix:  $E_m = 1$ . All phases considered isotropic with Poisson's ratio = 0.3.**

## CONCLUSIONS

A hurdle in modeling the behavior of nanotube-polymer composite systems is the non-bulk interphase region in these systems that forms due to nanoscale interactions between the embedded NTs and adjacent polymer chains. This interphase region comprises a substantial portion of the volume fraction of the composite due to the tremendous NT surface area per unit volume and results in significant changes in the viscoelastic properties of the nanotube-polymer composite compared to those of the bulk polymer. The micromechanical model developed here was motivated by the desire to model the effective mechanical behavior of these systems while maintaining an accurate physical representation of the annular interphase region surrounding the nanotubes, and particularly, in a manner suitable to model different orientational distributions of the coated nanotubes within the composite.

While the derivation and results presented here are for an elastic analysis, one can readily use the dynamic correspondence principle to extend this model for viscoelastic materials. In this regard the current model will be useful for inferring the change in mechanical properties of the interphase polymer based on macroscale experimental data for a particular nanotube-polymer system; such an approach may also be useful in characterizing the impact of various chemical functionalization strategies on interphase formation in nanocomposite systems. The present model may also find use for bridging atomistic simulations of nanotube-polymer systems with continuum-level predictions of the effective mechanical behavior of these materials.

## REFERENCES

1. Qian, D., G.J. Wagner, W.K. Liu, M.-F. Yu, and R.S. Ruoff, Mechanics of carbon nanotubes. *Applied Mechanics Reviews*, 55(6): p. 495-533, 2002.
2. Yakobson, B.I. and P. Avouris, Mechanical properties of carbon nanotubes, in *Carbon Nanotubes*, M.S. Dresselhaus, G. Dresselhaus, and P. Avouris, Editors. Springer-Verlag: Berlin Heidelberg. p. 287-327, 2001.
3. Lau, K.T., M. Chipara, H.Y. Ling, and D. Hui, On the effective elastic moduli of carbon nanotubes for nanocomposite structures. *Composites Part B Engineering*, 35(2): p. 95-101, 2004.
4. Fisher, F.T. and L.C. Brinson, Nanomechanics of Nanoreinforced Polymers, in *Handbook of Theoretical and Computational Nanotechnology*, M. Reith and W. Schommers, Editors. American Scientific Publishing, to be published.
5. Li, C.Y. and T.W. Chou, Multiscale Modeling of carbon nanotube reinforced polymer composites. *Journal of Nanoscience and Nanotechnology*, 3(5): p. 423-430, 2003.
6. Wei, C., D. Srivastava, and K. Cho, Thermal expansion and diffusion coefficients of carbon nanotube-polymer composites. *Nano Letters*, 2(6): p. 647-650, 2002.
7. Hu, N., H. Fukunaga, C. Lu, M. Makeyama, and B. Yan, Prediction of elastic properties of carbon nanotube reinforced composites. *Proceedings of the Royal Society of London Series A*, in press.
8. Jin, Z., K.P. Pramoda, G. Xu, and S.H. Goh, Dynamic mechanical behavior of melt-processed multi-walled carbon nanotube/poly(methyl methacrylate) composites. *Chemical Physics Letters*, 37: p. 43-47, 2001.
9. Park, C., Z. Ounaies, K.A. Watson, R.E. Crooks, J. Smith, S.E. Lowther, J.W. Connell, E.J. Siochi, J.S. Harrison, and T.L.S. Clair, Dispersion of single wall carbon nanotubes by in situ polymerization under sonication. *Chemical Physics Letters*, 364(3-4): p. 303-308, 2002.
10. Shaffer, M.S.P. and A.H. Windle, Fabrication and characterization of carbon nanotube/poly(vinyl alcohol) composites. *Advanced Materials*, 11(11): p. 937-941, 1999.
11. Fisher, F.T., A. Eitan, R. Andrews, L.S. Schadler, and L.C. Brinson, Spectral response and effective viscoelastic properties of MWNT-reinforced polycarbonate. *Advanced Composites Letters*, 13(2): p. 105-111, 2004.
12. Ding, W., A. Eitan, F.T. Fisher, X. Chen, D.A. Dikin, R. Andrews, L.C. Brinson, L.S. Schadler, and R.S. Ruoff, Direct observation of polymer sheathing in carbon nanotube-polycarbonate composites. *Nano Letters*, 3(11): p. 1593-1597, 2003.
13. Eitan, A., K. Jiang, R. Andrews, and L.S. Schadler, Surface modification of multi-walled carbon nanotubes: Towards the tailoring of the interface in polymer composites. *Chemistry of Materials*, 15(16): p. 3198-3201, 2003.
14. Eitan, A., F.T. Fisher, R. Andrews, L.C. Brinson, and L.S. Schadler, Reinforcement mechanisms in MWCNT-filled polycarbonate, 2005.
15. Mori, T. and K. Tanaka, Average stress in matrix and average elastic energy of materials with misfitting inclusions. *Acta Metallurgica*, 21: p. 571-574, 1973.
16. Benveniste, Y., A new approach to the application of Mori-Tanaka's theory in composite materials. *Mechanics of Materials*, 6: p. 147-157, 1987.
17. Weng, G.J., The theoretical connection between Mori-Tanaka's theory and the Hashin-Shtrikman-Wadpole bounds. *International Journal of Engineering Science*, 28(11): p. 1111-1120, 1990.
18. Chen, T., G.J. Dvorak, and Y. Benveniste, Mori-Tanaka estimates of the overall elastic moduli of certain composite materials. *Journal of Applied Mechanics*, 59: p. 539-546, 1992.
19. Tandon, G.P. and G.J. Weng, Average stress in the matrix and effective moduli of randomly orientated composites. *Composites Science and Technology*, 27: p. 111-132, 1986.
20. Luo, H.A. and G.J. Weng, On Eshelby's S-Tensor in a Three-Phase Cylindrically Concentric Solid, and the Elastic Moduli of Fiber-Reinforced Composites. *Mechanics of Materials*, 8: p. 77-88, 1989.
21. Fisher, F.T. and L.C. Brinson, Viscoelastic interphases in polymer matrix composites: Theoretical models and finite element analysis. *Composites Science and Technology*, 61(5): p. 731-748, 2001.
22. Fisher, F.T., Nanomechanics and the viscoelastic behavior of carbon nanotube-reinforced polymers, Ph. D. Thesis, Department of Mechanical Engineering, Northwestern University, 2002.
23. Benveniste, Y., G.J. Dvorak, and T. Chen, Stress fields in composites with coated inclusions. *Mechanics of Materials*, 7: p. 305-317, 1989.
24. Luo, H.A. and G.J. Weng, On Eshelby's Inclusion Problem in a Three-Phase Spherically Concentric Solid, and a Modification of Mori-Tanaka's Method. *Mechanics of Materials*, 8: p. 347-361, 1987.
25. Qui, Y.P. and G.J. Weng, Elastic moduli of thickly coated particle and fiber-reinforced composites. *Journal of Applied Mechanics*, 58: p. 388-398, 1991.
26. Bradshaw, R.D., F.T. Fisher, and L.C. Brinson, Fiber waviness in nanotube-reinforced polymer composites: II. Modelling via numerical approximation of the dilute strain concentration tensor. *Composites Science and Technology*, 63(11): p. 1705-1722, 2003.
27. Fisher, F.T. and K.C. Lee, Analytical solution for the dilute strain concentration tensor for coated fibrous inclusions, manuscript in preparation.